Food and Chemical Toxicology 171 (2023) 113542

Contents lists available at ScienceDirect

Food and Chemical Toxicology

journal homepage: www.elsevier.com/locate/foodchemtox

Hydroxytyrosol and dopamine metabolites: Anti-aggregative effect and neuroprotective activity against α-synuclein-induced toxicity

Marta Gallardo-Fernández, Ruth Hornedo-Ortega, Ana B. Cerezo, Ana M. Troncoso, M. Carmen Garcia-Parrilla *

Departamento de Nutrición y Bromatología, Toxicología y Medicina Legal, Facultad de Farmacia, Universidad de Sevilla, C/ Profesor García González nº 2, Sevilla, 41012, Spain

ARTICLE INFO

Handling Editor: Dr. Bryan Delaney

Keywords:
Hydroxytyrosol
Metabolites
Dopamine
α-synuclein
Neurotoxicity
Vitagenes

ABSTRACT

The abnormal aggregation of the α-synuclein (αsyn) protein is involved in the formation of Lewy bodies in the brain of patients suffering from Parkinson disease (PD). Hydroxytyrosol (HT), a polyphenolic compound present in olives, olive oil, and wine, has been shown to inhibit aggregation and destabilise the αsyn aggregates, preventing neuronal cell death. However, very limited data have been published on the study of its metabolites. Therefore, this study investigated the capacity of the metabolites 3,4-dihydroxyphenylacetaldehyde (DOPAL), 4-hydroxy-3-methoxyphenylethanol (MOPET), and 3-methoxy-4-hydroxyphenylacetaldehyde (MOPAL) to prevent the aggregation and toxic effects of αsyn fibrils. *In vitro* techniques, such as Thioflavin T (ThT), Transmission Electronic Microscopy (TEM), electrophoresis, thiazolyl blue tetrazolium bromide (MTT), and Real-Time PCR (RT-PCR) were used. Our results show that among these three metabolites, DOPAL exerts the greatest effect, preventing aggregation and αsyn-induced neurotoxicity. In fact, DOPAL has the ability to completely inhibit αsyn fibril formation at low doses. Moreover, this metabolite has a potent destabilising effect on the αsyn fibrils. Concerning neuroprotection, DOPAL can counteract the toxicity induced by αsyn. The vitagene expression results show a possible relationship between the neuroprotection mechanism exhibited by DOPAL and the modulation of SIRT-2 and Hsp70.

1. Introduction

Parkinson's Disease (PD) represents a devastating public health problem, being the second most common neurodegenerative disorder after Alzheimer's disease (AD) (Twelves et al., 2003). Indeed, more than 10 million people worldwide live with this disorder. The incidence of PD increases with age, but the number of people under 50 years of age who are diagnosed is currently increasing. The motor and neurological symptoms associated to this disorder dramatically reduce the quality of life and cause substantial cost to health systems, including drugs, rehabilitation, and caregiving (Dowding et al., 2006).

The histopathological hallmark of PD is the presence of intra-neuronal deposits containing fibrillar aggregates of the presynaptic protein αsyn, called Lewy bodies and Lewy neurites (Goedert, 2001). Although αsyn is expressed throughout the brain, the formation of these neurotoxic protein deposits causes the death of dopaminergic neurons in the *substantia nigra* (SN), suggesting a connection between αsyn fibril formation and dopamine (DA) metabolism (Xu et al., 2002; Mencacci et al., 2014). Thus, the search for molecules that may interfere with αsyn to inhibit fibril formation, and consequently neurotoxicity, represents one of the most promising preventive strategies for combating PD.

Another emerging approach to protecting brain cells from αsyn-induced neurotoxicity is to control the associated cellular stress (Calabrese et al., 2004, 2009; Trovato Salinaro et al., 2014). In this context, vitagenes refer to a group of genes that are strictly involved in preserving cellular homeostasis during stressful conditions. Vitagenes include sirtuins (SIRT), heat shock proteins (Hsp), and heme oxygenase-1 (HO-1), among others (Calabrese et al., 2010; Srivastava and Haigis, 2011).

In vitro and *in vivo* data support the fact that an increase in SIRT-1 activity protects against amyloid-β toxicity, preventing neurodegeneration (Kim et al., 2007). Furthermore, SIRT-1 can inhibit the phosphorylation of αsyn, reducing the formation of aggregates. In fact, a low level of accumulation of basal phosphorylated-αsyn was observed when SIRT-1 is overexpressed (Singh et al., 2017). On the other hand,

* Corresponding author.
E-mail addresses: mgfernandez@us.es (M. Gallardo-Fernández), rhornedo@us.es (R. Hornedo-Ortega), acerezo@us.es (A.B. Cerezo), amtroncoso@us.es (A.M. Troncoso), mcparrilla@us.es (M.C. Garcia-Parrilla).

https://doi.org/10.1016/j.fct.2022.113542
Received 3 August 2022; Received in revised form 10 November 2022; Accepted 27 November 2022
Available online 1 December 2022

Abbreviations

AD	Alzheimer's disease
ADH	alcoholdehydrogenase
ALP	autophagy-lysosomal pathway
ALR	aldehyde/aldose reductase
A.U.	arbitrary units
BBB	Blood Barrier Brain
COMT	catechol-O- methyl transferase
DA	dopamine
DMEM	Dulbecco's modified Eagle's medium
DMSO	dimethyl sulfoxide
DOPAL	3,4-dihydroxyphenylacetaldehyde
HO-1	heme oxygenase-1
Hsp	heat shock proteins
HT	hydroxytyrosol
MAO	monoamine oxidase
MOPAL	3-methoxy-4-hydroxyphenylacetaldehyde
MOPET	4-hydroxy-3-methoxyphenylethanol
MTT	thiazolyl blue tetrazolium bromide
Nrf2	nuclear factor erythroid 2–related factor 2
PBS	phosphate-buffered saline
PD	Parkinson disease
RT-PCR	Real-Time PCR
SD	standard deviation
SIRT	sirtuins
SN	substancia nigra
TEM	Transmission Electronic Microscopy
ThT	Thioflavin T
UPS	ubiquitin-proteasome system
αsyn	α-synuclein

Outeiro et al. (2007) reported that the inhibition of SIRT-2 gene expression could be useful for therapeutic intervention in PD since αsyn-mediated toxicity was observed only in cells with increasing levels of SIRT-2. In addition, the HO-1 enzyme exerts a neuroprotective role by degrading the intracellular levels of the pro-oxidant heme and by producing biliverdin, the precursor of bilirubin, the latter being an endogenous molecule with powerful antioxidant characteristics (Mancuso, 2004). Finally, the expression of Hsp, including protein chaperones, is essential for the folding and repair of damaged proteins, thus serving to promote cell survival conditions that would otherwise result in apoptosis (Morimoto, 2014). Hsp are classified according to their molecular weight, the 70 kDa family of stress proteins being one of the most extensively studied (Macario and De Macario, 2007). Specifically, their overexpression suppresses the toxicity of aberrantly folded αsyn protein (Jones et al., 2014).

A lower incidence of PD was observed in Mediterranean countries, this being related to a close adherence to their dietary pattern characterised by a high consumption of fruit and vegetables rich in polyphenolic compounds (Giovanni et al., 2009; Scarmeas et al., 2009; Alcalay et al., 2012). Among these bioactives, hydroxytyrosol (HT) is one of the main characteristic compounds present in olive oil, olives, and wine (Vissers et al., 2002). The mean free HT content in these foodstuffs is 5.2 μg/g in olive oils (Othman et al., 2009; Cioffi et al., 2010; Kesen et al., 2013), 629.1 μg/g in olives (Pereira et al., 2006; Ambra et al., 2017; Johnson et al., 2018), and 2.1 μg/mL in wine (Di Tommaso et al., 1998; Proestos et al., 2005; Boselli et al., 2006; Piñeiro et al., 2011).

In addition, HT is also a DA metabolite, being endogenously synthesised in humans (Meiser et al., 2013; Rodríguez-Morató et al., 2016). Therefore, the biological effect of HT largely depends on its bioavailability and metabolization, similar to many polyphenol metabolites, presenting a different activity than their parent compounds (Lambert et al., 2007; Larrosa et al., 2009; Hornedo-Ortega et al., 2022). The low concentration of circulating HT is likely due to phase I and II metabolism in the gut and liver (Rodríguez-Morató et al., 2016). The enzymes involved in HT phase I metabolism are mostly present in the intestinal wall. They are non-microsomal alcohol and aldehyde dehydrogenases, both located in the cytosol, which synthesise metabolites such as 3,4-dihydroxyphenylacetaldehyde (DOPAL). DOPAL is also a DA metabolite by deamination (Rodríguez-Morató et al., 2016). Furthermore, 4-hydroxy-3-methoxyphenylethanol (MOPET) and 3-methoxy-4-hydroxyphenylacetaldehyde (MOPAL) are two other compounds related to the metabolism of HT and DA, respectively (Muñoz et al., 2012; Monzani et al., 2019). MOPET is a methylated metabolite of HT (also identified in olive oil) (Rodríguez-Morató et al., 2016) and MOPAL is the methylated metabolite of DOPAL. Therefore, although DOPAL, MOPET, and MOPAL can be considered dietary metabolites of HT, their plasmatic levels are not specific to HT, since they are also produced from DA metabolism.

Wu et al. (2009) have demonstrated that HT can cross the blood-brain barrier (BBB), being 13.6 μM the maximum concentration in the brain after an intravenous administration of 100 mg/kg weight in rats. The physiological concentrations of DA in the nervous system and bodily fluids are lower, ranging between 0.1 and 1.5 μM (Burke et al., 1999). Very few studies have been published on HT and DA metabolites. Physiological HT phase II metabolite concentration (sulphates) is estimated at 10 μM (López de las Hazas et al., 2016). Regarding DOPAL, the human brain tissue concentration was previously reported at 2.3 μM (Burke et al., 1999). Nevertheless, physiological concentrations of MOPET and MOPAL have not been described in the literature as far as we know.

Recently, it has been shown that HT can interact with the αsyn protein, inhibiting its aggregation and protecting neuronal PC12 cells (Hornedo-Ortega et al., 2018; Palazzi et al., 2020) by increasing the expression of some vitagenes (SIRT-2, HO-1, Hsp70) (Gallardo-Fernández et al., 2019). Furthermore, *in vivo* studies have demonstrated that HT exerts a potent antioxidant effect in the 1-methyl-4-phenylpyridinium-induced oxidative stress model of PD in rats, preserving striatal cells from DA depletion and attenuating the behavioural alterations (Pérez-Barrón et al., 2021). Moreover, using a rotenone-stressed PD-model of *Caenorhabditis elegans,* HT prevented neurodegeneration and improved locomotor behaviour (Brunetti et al., 2020). However, very few studies have been published regarding the neuroprotective activity of HT metabolites. Very recently, DOPAL (0.5 or 1 mM) was shown to stabilize toxic oligomers of αsyn through the oxidation of methionine residues of αsyn, thus playing an important role in preventing the progression of PD (Carmo et al., 2018). Indeed, other authors showed that DOPAL is a potent toxic compound for neurons (Kristal et al., 2001). However, Goldstein (2020) very recently highlighted that the interactions between DOPAL and αsyn are not well understood, revealing the need for further research.

DOPAL, MOPET, and MOPAL could contribute to modulation of the activity of HT. Therefore, knowledge of their effects could contribute to a better understanding of the bioactivity of HT. Thus, this study focuses on the properties of these three metabolites against αsyn aggregation and toxicity in PC12 cells. Additionally, the effect of these compounds on the vitagene system was evaluated.

2. Materials and methods

2.1. Chemicals and reagents

DOPAL (Purity: ≥90%) was acquired from Cayman Chemical (Ann Arbor, MI, USA). MOPAL (99%), MOPET (99%), Thioflavin T (ThT),

SIRT-1, SIRT-2, Hsp70, HO-1, and β-actin primers (Table 1), trypsin-EDTA, Dulbecco's modified Eagle's medium (DMEM)-high glucose, thiazolyl blue tetrazolium bromide (MTT), phosphate-buffered saline (PBS), L-glutamine, foetal horse serum, foetal bovine serum, penicillin/streptomycin, and dimethyl sulfoxide (DMSO) were obtained from Sigma–Aldrich (St. Louis, MO, USA).

PC12 cells were obtained from the American Type Culture Collection (ATCC) (Manassas, VA, USA). Human recombinant αsyn protein was purchased from Alexotech (Umeå, Sweden). 2-mercaptoethanol, 10X Tris/glycine/SDS (10X premixed electrophoresis buffer containing(25 mM Tris, 192 mM glycine, 0.1% SDS, at pH 8.3), 10X Tris/glycine (10X premixed electrophoresis buffer, pH 8.3), 4–20% Mini-PROTEAN TGX Stain-Free polyacrylamide gel, Immun-Blot PVDF membrane, and Coomassie Blue were bought from Bio Rad (Munich, Germany). Carbon-coated grids (300 mesh, copper) were supplied by EMS (Hatfield, PA, USA) and Revert Aid First Strand cDNA Synthesis Kit was obtained from Thermo Fisher Scientific (Waltham, MA, USA). TRIsure reagent and SensiFAST TM SYBR R® No-ROX Kit were purchased from Bioline (Swedesboro, NJ, USA).

2.2. ThT assay: Measurement of αsyn fibril formation and destabilisation

The method is based on the work published by Ono et al. (2012), adapted by our research group, using ThT as a fluorescent marker that binds to αsyn fibrils to monitor αsyn aggregation (Hornedo-Ortega et al., 2016, 2018a, 2018b; Gallardo-Fernández et al., 2019). For the inhibition assay, the αsyn monomers were prepared at 70 μM in Na_2HPO_4/-NaH_2PO_4 (25 mM)/NaCl buffer (pH 7.4). On the other hand, for the destabilisation assay, first, the αsyn monomers (70 μM) were incubated for 6 days on a thermoblock at 37 °C, under continuous agitation (1000 rpm) to form the αsyn fibrils. For both the inhibition and destabilisation assays, ThT (25 μM final concentration) was incubated with the αsyn monomers or pre-formed fibrils (70 μM) in the presence or absence of the individual compounds under study: DOPAL, MOPAL and MOPET at 20, 50, 100, and 150 μM in Na_2HPO_4/NaH_2PO_4 (25 mM)/NaCl buffer at 37 °C for 6 days (Hornedo-Ortega et al., 2018a, 2018b; Gallardo-Fernández et al., 2019) in black clear-bottomed 96-well plates. As for the incubation conditions, we used continuous agitation (1000 rpm) for the inhibition assay, whereas the destabilisation assay was performed without agitation.

Fluorescence emission data were recorded for 6 days using a multi-detector microplate reader fluorescence spectrophotometer (Synergy HT, Biotek) set at 450 nm for excitation and 485 nm for emission wavelengths. Samples were stored at −80 °C for the subsequent acquisition of Transmision Eletronic Microscopy (TEM) images and electrophoresis experiments.

2.3. TEM images

To obtain images of the state of aggregation of αsyn fibrils exposed to DOPAL, MOPAL, and MOPET, 10 μL of samples from each condition obtained in ThT assay were placed on a 300-mesh carbon-coated Formvard grid and incubated for 20 min. Afterwards, 5 μL of 2.5% (v/v) glutaraldehyde was placed on the grid and incubated for 5 min. Next, the grids were negatively stained for 1 min with 5 μL of 0.5% uranyl acetate solution. The excess fluid was removed, and the samples were viewed using a Zeiss Libra 120 TEM, operating at 80 kV.

2.4. Electrophoresis

To confirm the effect of the compounds under study on the inhibition of αsyn fibril formation and their disaggregation capacity, a total of 15 μL of the ThT samples was diluted with 5 μL of loading buffer. Then, the samples were heated at 50 °C for 3 min and loaded onto 4–20% Tris−glycine gel for 1 h at 100 V. Afterwards, the gels were stained with Coomassie Blue (0.1% Coomassie R250, 10% acetic acid, and 40% methanol).

2.5. PC12 cell culture

PC12 is an immortalised cell line derived from rat adrenal gland pheochromocytoma. The cells were grown in DMEM supplemented with 15% (v/v) foetal horse serum and 2.5% (v/v) foetal bovine serum, 100 μg/mL of penicillin and 100 μg/mL of streptomycin at 37 °C in an atmosphere of 5% carbon dioxide. The cells were detached with 1 × trypsin−EDTA every 3–4 days, the time needed to reach between 80 and 100% confluence.

2.6. MTT assay: cell cytotoxicity

To perform this assay, 30000 cells per well in 200 μL DMEM were cultured in 96-well plates for 24 h. Afterwards, the cells were exposed to DOPAL, MOPAL, or MOPET at 5, 10, 20, 50, 100, and 150 μM final concentrations dissolved in DMEM. These concentrations were selected in agreement with the HT concentrations used in our previous works for the sake of comparison (Hornedo-Ortega et al., 2018; Gallardo-Fernández et al., 2019). Furthermore, DMEM at 0.01% DMSO was used as a negative control. The cells were incubated with the individual compounds for 24 h at 37 °C. Later, the cells were treated with 200 μL MTT solution per well (final concentration, 0.5 mg/mL in DMEM) for 3 h at 37 °C with 5% CO_2. The purple crystals formed were solubilised with 100 μL of DMSO per well for 30 min in the dark. Finally, the absorbance was measured at 540 and 570 nm with a microplate reader (Synergy HT, Biotek) using a reference wavelength of 630 nm.

2.7. Neuroprotective assays

DOPAL (20, 50, 100, and 150 μM) and MOPET (100 and 150 μM) were mixed in individual tubes with αsyn monomers (70 μM) in phosphate buffer. Similarly, the αsyn monomers (70 μM) were incubated alone (positive control). Then, they were incubated for 6 days on a thermoblock at 37 °C under continuous agitation (1000 rpm). Afterwards, these solutions were diluted with DMEM to reach a final concentration of 7 μM for the αsyn fibrils in accordance with previous studies (Hornedo-Ortega et al., 2018a, 2018b), and mixed with DOPAL (2, 5, 10, and 15 μM) or MOPET (10 and 15 μM final concentration). These solutions were placed in contact with PC12 cells and incubated for 24 h. Afterwards, MTT was carried out as was explained above.

2.8. RT-PCR analysis

PC12 cells were seeded in 24-well plates for 24 h at 37 °C, and then treated with and without αsyn fibrils (7 μM) plus DOPAL and MOPET (0.5, 2, 5, 10, and 15 μM), and MOPAL (0.5 μM). Total RNA after the different treatments was extracted from the PC12 cells using TRIsure reagent. Next, 1 μg of total RNA was transformed into cDNA using the RevertAid First Strand cDNA Synthesis Kit as described by the manufacturer. RT-PCR was performed using 5 μL of the SensiFAST TM SYBR NO-ROX KIT, 0.4 μL of each primer, and 4.2 μL cDNA for a final reaction volume of 10 μL in 384-well plates. Amplification was run in a Lightcycler® 480 Instrument II (Roche, Rotkreuz, Switzerland): thermal cycler at 95 °C for 2 min, followed by 40 cycles consisting of a denaturation phase for 5 s at 95 °C, a second hybridization phase at 65 °C for 10 s, and a final elongation phase at 72 °C for 20 s. The process was completed by a final step consisting of 7 min at 72 °C. Analysis confirmed a single PCR product. β-actin served as reference gene and was used for sample normalization. The primer sequences for SIRT-1, SIRT-2, Hsp70, and HO-1 are shown in Table 1 (supplementary materials).

2.9. Statistical analysis

Statistical analysis was performed using Graphpad Prism 6.01 software (GraphPad Software, Inc., San Diego, CA, USA), using one-way analysis of variance (ANOVA test) to explore significant differences ($p < 0.05$). Data are displayed as mean ± standard deviation (SD).

3. Results

3.1. MOPET, MOPAL and DOPAL's effect on αsyn fibril formation

The ThT fluorescence assay was used to evaluate whether MOPET, MOPAL, and DOPAL (Fig. 1) could inhibit αsyn fibril formation. This assay was selected because fluorescence increases in the presence of misfolded fibrils. Fig. 2A shows the kinetics of αsyn aggregation with and without MOPET, MOPAL, and DOPAL for 6 days. When αsyn was incubated alone, the fluorescence signal progressively increased with time until it reached the maximum fluorescence on days 5 and 6 (Fig. 2A). However, when αsyn was incubated with MOPET at 100 and 150 μM or with DOPAL at 20, 50, 100, and 150 μM, ThT fluorescence diminished significantly indicating lower αsyn fibril formation (Fig. 2A–C). On the other hand, no effect against αsyn fibril formation was observed for MOPAL at any concentration tested. It is worth mentioning that complete inhibition of fibril formation (102% ± 13) was reached by DOPAL at 20 μM, which was the lowest concentration tested (Table 1). Conversely, for concentrations greater than 100 μM, the percentage of inhibition was lower, thus demonstrating a non-dose-dependent effect that was inversely proportional to the dose. In the case of MOPET, we could only see a significant effect at 100 and 150 μM, showing very similar inhibition percentages (45 and 55%, respectively) (Table 1).

TEM images confirmed the inhibitory effect of DOPAL and MOPET (Fig. 2B–H). Fig. 2B shows that when αsyn was incubated alone, αsyn fibrils were formed (Fig. 2B). The co-incubation of DOPAL with αsyn showed that the amount of αsyn aggregates increases as DOPAL concentration increases (Fig. 2C–F). Only small amorphous aggregates were observed in Fig. 2C corresponding to DOPAL at 20 μM. In the case of MOPET, the number of aggregates clearly diminished at 100 and 150 μM (Fig. 2G–H).

The separation of proteins by electrophoresis allowed us to verify the previous findings, based on the protein size of αsyn after 6 days of incubation with and without the compounds under study (Fig. 2I). The reported molecular weights corresponding to the monomers and dimers are 14.5 and between 24 and 63 KDa, respectively (Winner et al., 2011; Ardah et al., 2014). Therefore, the bands corresponding to αsyn alone appeared at 14.5 KDa (monomers), 25, and 40 KDa (dimers) (Fig. 2I). In the presence of MOPET (100 and 150 μM) and DOPAL (20, 50, 100, and 150 μM), the bands corresponding to the αsyn dimers and trimers presented a weaker intensity than the band for αsyn alone, proving the inhibitory effect of both compounds on αsyn fibril formation. As previously showed by the ThT assay, the electrophoresis images also prove that DOPAL affects αsyn formation differently according to its concentration. Thus, we can observe the presence of bands corresponding to monomers, dimers, and trimers (15, 25, and 40 KDa, respectively) when DOPAL at 150 μM was co-incubated with αsyn. Conversely, when DOPAL was present at 20, 50, and 100 μM, we observed an absence of the bands corresponding to the dimers and trimers (Fig. 2I).

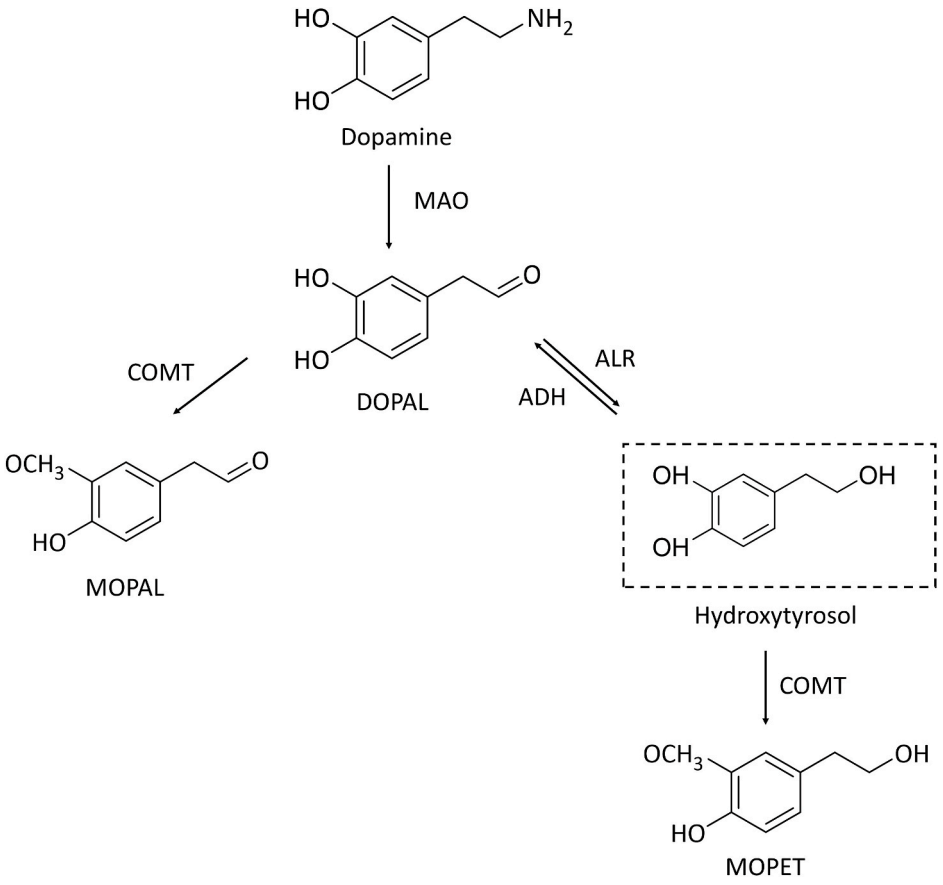

Fig. 1. Dopamine and hydroxytyrosol metabolic pathways in humans. MAO: monoamine oxidase; COMT: catechol-*O*-methyl transferase; ALR: aldehyde/aldose reductase; ADH: alcohol dehydrogenase.

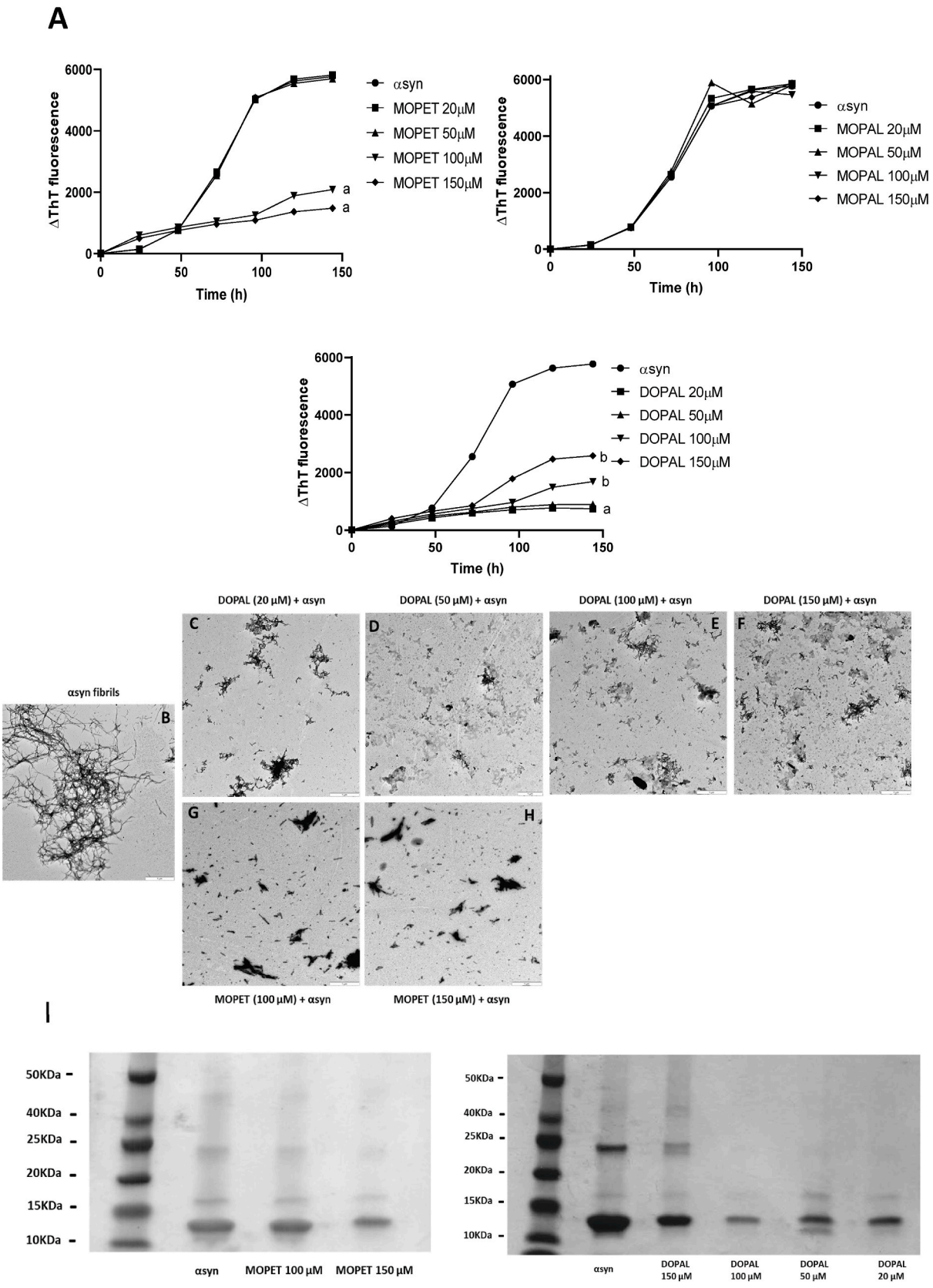

Fig. 2. A: Effects of MOPET, MOPAL, and DOPAL (20, 50, 100, and 150 μM) on inhibition of αsyn fibril formation measured by ThT fluorescence at λEx 450 and λEm 485. a: $p < 0.0005$ *versus* αsyn; b: $p < 0.005$ *versus* αsyn. TEM images. B: αsyn fibrils; C: DOPAL (20 μM) + αsyn fibrils; D: DOPAL (50 μM) + αsyn fibrils; E: DOPAL (100 μM) + αsyn fibrils; F: DOPAL (150 μM) + αsyn fibrils; G: MOPET (100 μM) + αsyn fibrils H: MOPET (150 μM) + αsyn fibrils. Electrophoresis. I: Samples from the ThT assay (inhibition) were separated with 4–20% Tris−glycine SDS gel and stained with Coomassie Blue. All experiments were performed in triplicate ($n = 3$).

Table 1
Inhibition and destabilisation percentages for MOPET, MOPAL, and DOPAL against αsyn fibrils ($n = 3$).

Compound	Concentration (μM)	% Inhibition ± SD	% Destabilisation ± SD
DOPAL + αsyn	20	102 ± 13	43 ± 8
	50	93 ± 5	71 ± 6
	100	70 ± 3	78 ± 5
	150	67 ± 9	80 ± 3
MOPAL + αsyn	20	n.d.	n.d.
	50	n.d.	n.d.
	100	n.d.	n.d.
	150	n.d.	n.d.
MOPET + αsyn	20	n.d.	n.d.
	50	n.d.	n.d.
	100	45 ± 7	n.d.
	150	55 ± 2	3 ± 2

n.d. not detected, SD standard deviation.

3.2. MOPET, MOPAL, and DOPAL's effect on the destabilisation of pre-formed αsyn fibrils

The objective of the ThT assay was to evaluate whether these metabolites could destabilise the pre-formed αsyn fibrils. As shown in Fig. 3A, DOPAL was the only compound which reduced the level of αsyn fibrils in a dose-dependent manner. Indeed, we obtained the following destabilisation percentages: 43, 71, 78, and 80% for 20, 50, 100, and 150 μM, respectively (Table 1). Additionally, the TEM images displayed in Fig. 3C–F shows a decrease in the number of αsyn fibrils as the DOPAL concentration increases. On the other hand, Fig. 3G reveals that MOPET (150 μM) does not present a destabilising effect since we can observe a high number of αsyn fibrils. Furthermore, all these results are supported by the electrophoresis assay (Fig. 3H). Both the monomer and dimer bands were present in the MOPET samples as well as in the control containing αsyn alone, confirming that this metabolite does not present any destabilising effect. Regarding DOPAL, the bands corresponding to the αsyn dimers and trimers were only present in αsyn alone and DOPAL samples at 20 μM. On the contrary, higher DOPAL concentrations (50–150 μM) showed an absence of bands for αsyn dimers and trimers, which proves the destabilising potential of DOPAL from concentrations of 50 μM (Fig. 3H).

3.3. MOPET and DOPAL maintain the viability of PC12 cells

The cytotoxicity of DOPAL, MOPAL, and MOPET at different concentrations (5, 10, 20, 50, 100, and 150 μM) was studied to select the non-cytotoxic concentration for the subsequent experiments (Fig. 4). Fig. 2 displays the percentage of cell viability for each compound, showing no toxic effect for DOPAL and MOPET at every tested concentration. However, MOPAL was significantly toxic for PC12 cells from 20 μM.

3.4. MOPET and DOPAL reduce αsyn toxicity on PC12 cells

The neuroprotective effect of MOPET and DOPAL in PC12 cells against the toxicity induced by αsyn fibrils was evaluated by the MTT assay (Fig. 5A–B). The concentrations tested were selected according to the ThT results. In this case the concentrations of both αsyn and compounds were reduced ten-fold in order to compare the results obtained by both assays. After treating PC12 cells with MOPET at 15 μM, we can see a significant increase of 30% in cell viability compared with cells incubated only with αsyn. In the same way, cell viability was significantly enhanced in the presence of DOPAL (2, 5, 10, and 15 μM), being 2 and 5 μM the most effective concentrations since they increase cell viability by 45%.

3.5. Effects of MOPET, MOPAL, and DOPAL on SIRT-1, SIRT-2, Hsp 70, and HO-1 gene expression

For a more complete picture of the activity of MOPET and DOPAL, we considered the gene expression of SIRT-1, SIRT-2, Hsp70, and HO-1, which are genes involved in the vitagene system (Fig. 6A–H). Furthermore, the effect of MOPAL on vitagene expression was also assayed. For every gene under study, two controls were performed (untreated cells and cells incubated with αsyn alone). As can be observed in Fig. 6A, DOPAL (0.5, 5, and 15 μM) and MOPET (0.5, 5, 10, and 15 μM) in the absence of αsyn fibrils significantly increased SIRT-1 gene expression. However, when the compounds were incubated with αsyn fibrils (7 μM), the expression of this gene was maintained and significant differences were only observed when the cells were incubated with DOPAL at 15 μM (Fig. 6B). In addition, in the case of SIRT-2 and HO-1 gene expression, a significant decrease occurred in all the conditions tested with and without αsyn fibrils (Fig. 6C–F). It is remarkable that the condition that produced the greatest decrease in SIRT-2 gene expression was MOPAL at 0.5 μM, incubated in the absence of αsyn fibrils, with an expression value that was 98 times less than the control (Fig. 6C). Conversely, DOPAL at 5 μM produced the most significant decrease in HO-1 gene expression (Fig. 6E). All the conditions tested in the absence of αsyn fibrils produced a significant increase of up to 500 times greater as compared to the control for Hsp70 gene expression (Fig. 6G). Finally, a significant increase in Hsp70 expression was also observed for DOPAL at 5 μM and for MOPET at 10 μM in the presence of αsyn fibrils but to a lower extent (Fig. 6H).

4. Discussion

Neurodegeneration is considered one of the reasons for disease progression in PD. The factors that initiate neurodegeneration are oxidative stress, neuroinflammation, and abnormal αsyn aggregations among others (Fahn and Sulzer, 2004; Aaseth et al., 2018). A substantial body of evidence suggests that the modulation of αsyn aggregation by small molecules such as polyphenolic compounds can be a potential strategy against the development and progress of PD (Bieschke et al., 2010; Hornedo-Ortega et al., 2018a, 2018b; Palazzi et al., 2018; Gallardo-Fernández et al., 2019).

In this work, we studied the effects of HT and DA metabolites, namely MOPET, MOPAL, and DOPAL against the aggregation and disaggregation of αsyn fibrils and the study of vitagene expression as part of their potential mechanism of action.

We present evidence that the HT metabolite MOPET at concentrations of 100 and 150 μM is effective at inhibiting αsyn fibril formation by 45 and 55%, respectively (Fig. 2A, Table 1). However, when αsyn fibrils are already being formed, MOPET has no effect on the destabilisation of the αsyn fibrils (Fig. 3A). On the other hand, MOPAL has no effect against αsyn fibril formation and destabilisation (Figs. 2A and 3A, respectively). This difference in activity for MOPET and MOPAL may be explained by their different chemical structures. In fact, another study carried out in our laboratory demonstrated that HT presented a more potent inhibitory (81%, 100 μM) and destabilising (63%, 100 μM) activity against αsyn fibril formation (Hornedo-Ortega et al. 2018) than MOPET (100 μM). MOPET differs from HT in the methylation of one of the hydroxyl groups attached to the benzene ring. Regarding MOPAL, it presents two modifications with respect to HT: it contains one methoxy group instead of one of the hydroxyl groups and an aldehyde instead of an –OH group in the chain attached to the benzene ring, which decreases the electron density of the ring and, in turn, its activity (Fig. 1).

Additionally, we tested DOPAL. The concentration at which this metabolite has an effect against αsyn fibril aggregation depends on the state of the protein. Interestingly, we observed that the results obtained for DOPAL follow an uncommon pattern. In fact, when DOPAL was incubated with αsyn monomers, we observed that its inhibitory effect against αsyn fibril formation depended inversely on the DOPAL

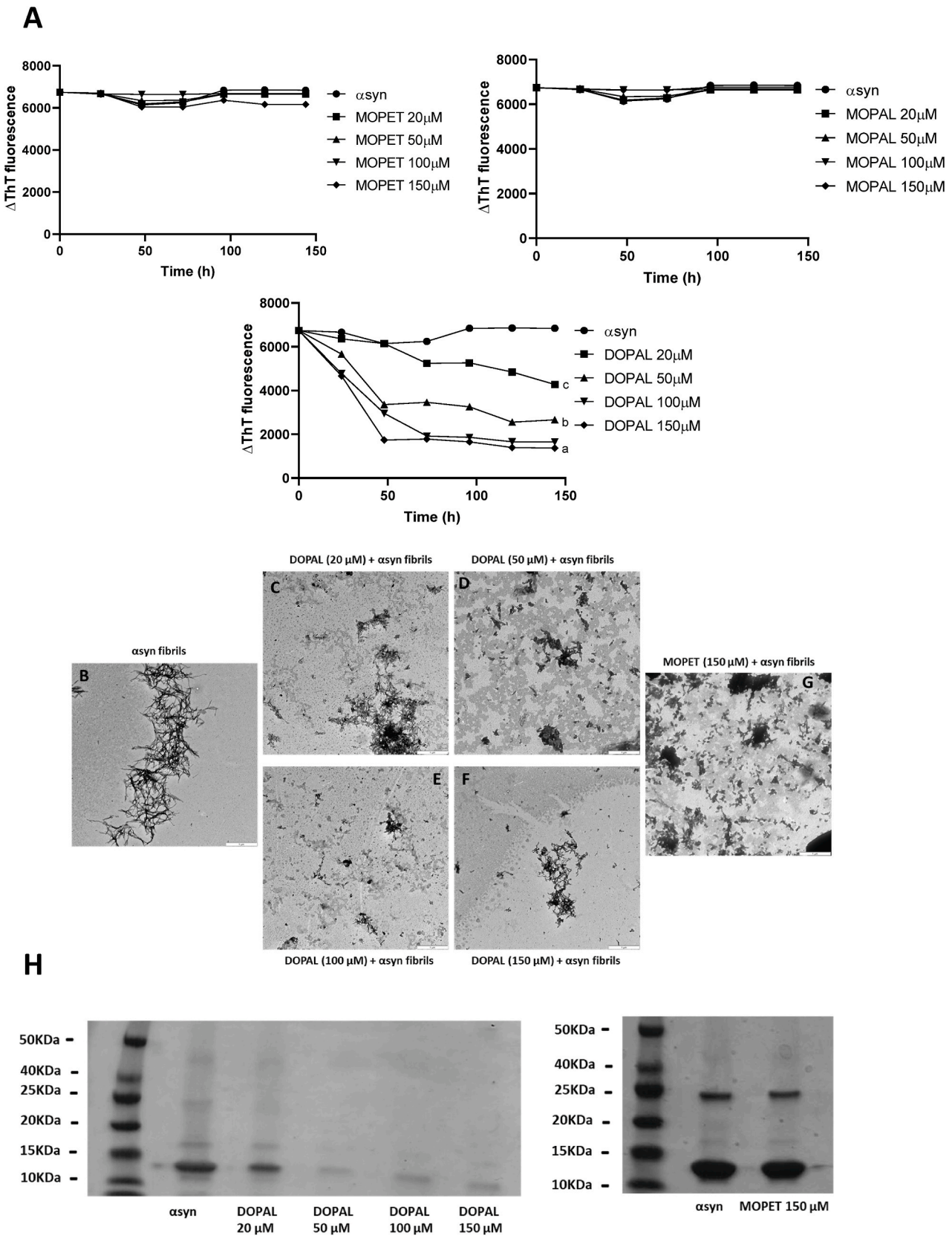

Fig. 3. A: Effects of MOPET, MOPAL, and DOPAL (20, 50, 100, and 150 μM) on destabilisation of αsyn fibrils measured by ThT fluorescence at λEx 450 and λEm 485. a: $p < 0.0005$ *versus* αsyn; b: $p < 0.005$ *versus* αsyn; c: $p < 0.05$ *versus* αsyn. TEM images. B: αsyn fibrils; C: DOPAL (20 μM) + αsyn fibrils; D: DOPAL (50 μM) + αsyn fibrils; E: DOPAL (100 μM) + αsyn fibrils; F: DOPAL (150 μM) + αsyn fibrils; G: MOPET (150 μM) + αsyn fibrils. Electrophoresis. H: Samples from the ThT assay (destabilisation) were separated with 4–20% Tris−glycine SDS gel and stained with Coomassie Blue. All experiments were performed in triplicate ($n = 3$).

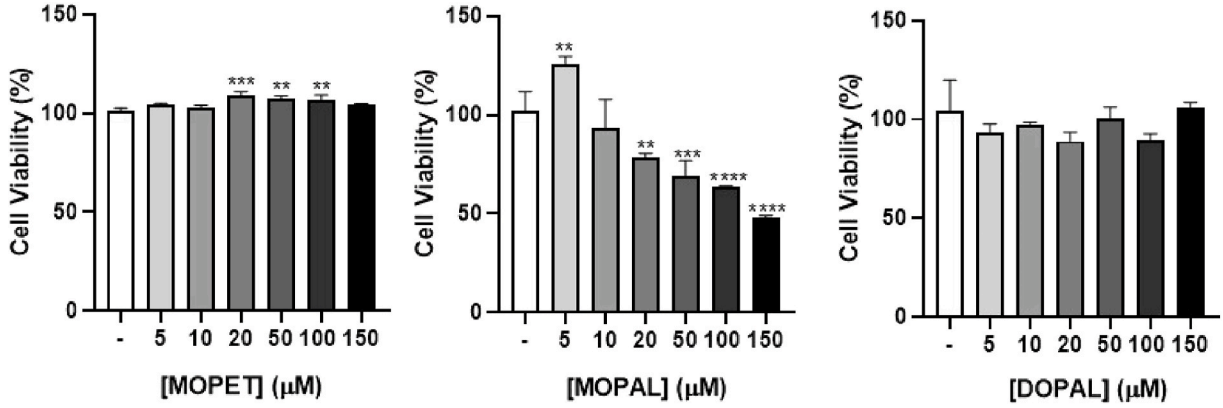

Fig. 4. Cell viability (%) (MTT assay) in PC12 cells for MOPET, MOPAL, and DOPAL (5, 10, 20, 50, 100, 150 μM). Results are expressed as mean ± standard deviation (SD) of three analytical replicates ($n = 3$). $^{**}p < 0.005$, $^{***}p < 0.0005$, $^{****}p < 0.00005$ compounds *versus* control (−).

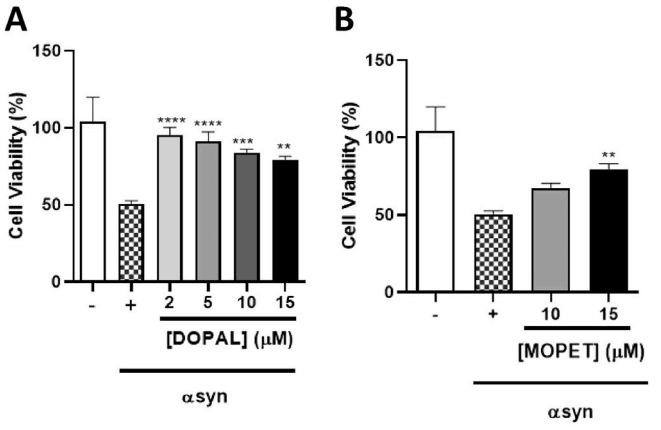

Fig. 5. Cell viability (%) (MTT assay) of PC12 cells in presence of A: DOPAL (2, 5, 10, and 15 μM) and B: MOPET (10 and 15 μM) with 24h pre-treatment against α-syn toxicity (7 μM). Data are expressed as mean ± standard deviation (SD) of three analytical replicates ($n = 3$). $^{**}p < 0.005$, $^{***}p < 0.0005$, $^{****}p < 0.00005$ compounds *versus* αsyn control (−).

concentrations. At lower concentrations, a greater inhibitory effect was observed (Fig. 2A and Table 1). TEM images confirm the presence of αsyn fibrils in the case of DOPAL at 150 μM (Fig. 3F) and αsyn monomers at 20 μM (Fig. 2C). In accordance with our results, Burke et al. (2008) observed that as DOPAL concentration increases, the molecular weight of the αsyn aggregates also increases. It is worth highlighting the conditions used in both papers. In fact, Burke et al. (2008) tested DOPAL concentrations ranging between 1.5 and 1000 μM and used an αsyn concentration of 2 μM, which is remarkably higher than our DOPAL-αsyn ratio (150-70 μM). Another difference was the incubation time; in our case we incubated the DOPAL-αsyn mix for 6 days. However, in the Burke et al. (2008) study, this period was only 4 h. All in all, the differences observed can be explained by the difference in study conditions. Moreover, more recently Plotegher et al. (2017) used ThT and TEM to demonstrate that the incubation of αsyn with DOPAL (1:16) inhibits αsyn fibril formation, which is closely related with our results obtained for a 1:2 ratio (αsyn: DOPAL). This inhibitory effect on αsyn fibril formation can be explained by the formation of covalent adducts between DOPAL and the N-terminal lysine residues of αsyn. This interaction has been associated with the stabilisation of αsyn oligomers by DOPAL, avoiding the formation of future αsyn fibrils (Follmer et al., 2015; Werner-Allen et al., 2016; Plotegher et al., 2017; Lima et al., 2018). Furthermore, Carmo-Gonçalves et al. (2018) demonstrated that the oxidation of all four methionine residues of the αsyn monomer reduces the protein's ability to form large oligomers in the presence of DOPAL (Carmo-Gonçalves et al., 2018). In summary, these findings indicate that lysine and methionine residues may have an important role in driving the oligomerisation of DOPAL-derived αsyn species (Follmer et al., 2015; Werner-Allen et al., 2016; Plotegher et al., 2017; Carmo--Gonçalves et al., 2018).

Regarding destabilisation, our results prove that DOPAL follows a dose-dependent effect when this compound is incubated with preformed αsyn fibrils and can destabilise the αsyn fibrils by 80% at the maximum DOPAL concentration tested (150 μM) (Fig. 3A, Table 1). Previous studies by our group have shown that HT exerts a significant destabilising effect (around 65%) (Hornedo-Ortega et al., 2018a), similar to those reported here for DOPAL.

Our work was undertaken to compare the effects of different molecules with previously published data under identical conditions (Hornedo-Ortega et al., 2018a). The selected metabolites are related via DA metabolism and some of them are present in dietary sources. Little is known about the enzymes that interconvert these metabolites, which might have a role in the extent they are present *in vivo*. These enzymes may transform HT into DOPAL or the other way round.

The most relevant biological consequence of misfolded αsyn association is the production of neurotoxic structures that finally cause cell death (Ardah et al., 2014; Steiner et al., 2011). Considering its extensive metabolism (Rodríguez-Morató et al., 2016), our objective was to evaluate the toxicity of HT metabolites in plasma and brain at physiological concentrations (0.1–10 μM) (Burke et al., 1999; Kristal et al., 2001; López de las Hazas et al., 2016; 2018).

Regarding the neuroprotective effect of the evaluated metabolites, our results show that DOPAL (2, 5, 10, and 15 μM) and MOPET (10 and 15 μM) are effective against αsyn-induced toxicity (Fig. 5A–B), preventing PC12 cell death in part due to their ability to inhibit the formation of αsyn fibrils in the same way as the inhibition assay. In this context, Carmo-Gonçálvez et al. (2020) reported that DOPAL-derived αsyn adducts exhibited lower toxicity compared with DOPAL itself, raising the question of whether the generation of these adducts could be part of or a collateral effect of αsyn-mediated protection in neurons exposed to DOPAL (Carmo-Gonçálvez et al., 2020).

Previous studies have shown that HT, the precursor of the metabolites DOPAL and MOPET, at 10 μM reverses (15–20%) the toxic effect produced by αsyn to an extent similar to that of MOPET (Hornedo-Ortega et al., 2018a). However, our results prove that DOPAL (10 μM) is more effective that MOPET and HT, increasing viability by around 40% (Fig. 5).

Furthermore, modulation of endogenous cellular defence mechanisms represents an innovative approach to therapeutic intervention in diseases causing chronic tissue damage, such as neurodegeneration (Calabrese et al., 2010). To elucidate the possible mechanism of action of MOPET and DOPAL, we proved their effect on SIRT-1, SIRT-2, Hsp70,

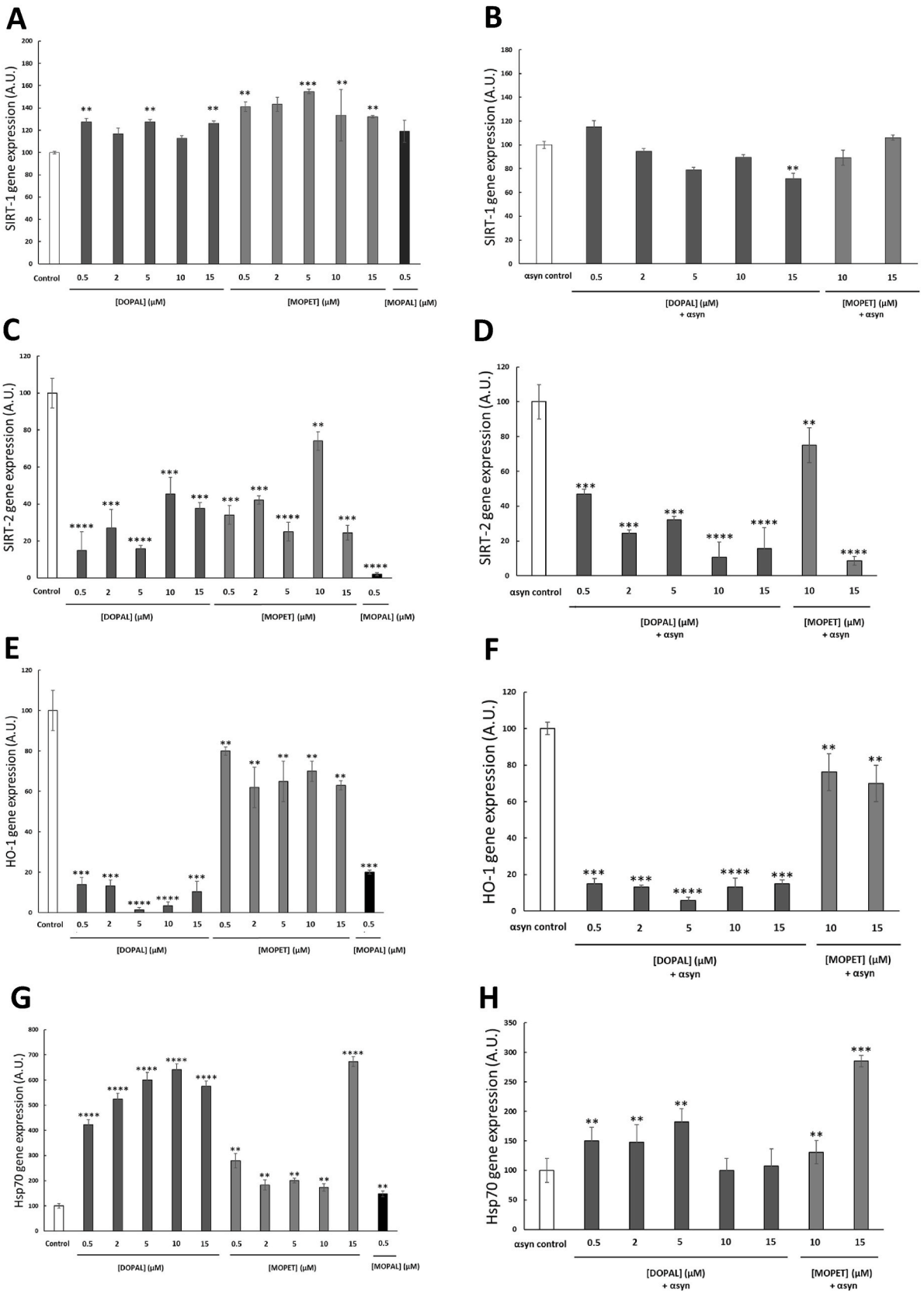

Fig. 6. DOPAL (0.5, 2, 5, 10, and 15 μM), MOPET (0.5, 2, 5, 10, and 15 μM) and MOPAL (0.5 μM) effect on vitagene expression. A: SIRT-1 gene expression (A.U.) without αsyn; B: SIRT-1 gene expression (A.U.) with αsyn (7 μM); C: SIRT-2 gene expression (A.U.) without αsyn; D: SIRT-2 gene expression (A.U.) with αsyn (7 μM); E) HO-1 gene expression (A.U.) without αsyn; F: HO-1 gene expression (A.U.) with αsyn (7 μM); G) Hsp 70 gene expression (A.U.) without αsyn; H: Hsp 70 gene expression (A.U.) with αsyn (7 μM). Data are expressed as mean ± standard deviation (SD) ($n = 3$). $^{**}p < 0.005$, $^{***}p < 0.0005$, $^{****}p < 0.00005$ compounds *versus* control.

and HO-1 gene expression in PC12 cells. Furthermore, we considered the effect of MOPAL on vitagene expression in PC12 cells.

Our results show that in the absence of αsyn fibrils, DOPAL at 0.5, 5, and 15 μM and MOPET at 5, 10, and 15 μM significantly increase SIRT-1 gene expression, with MOPET at 5 μM exhibiting the highest SIRT-1 expression in the absence of αsyn fibrils (Fig. 6A). Indeed, increased SIRT1 levels and its activation have been reported as beneficial in acute neuronal injuries (Gao et al., 2012), and in a great range of neurodegenerative diseases (Srivastava and Haigis, 2011; Ng et al., 2015). On the other hand, in the presence of αsyn fibrils, DOPAL at 15 μM cannot counteract the significant decrease in SIRT-1 gene expression produced in the presence of αsyn fibrils alone (Fig. 6B).

In addition, our results showed that for all the conditions tested DOPAL and MOPET produced a potent inhibition of SIRT-2 gene expression (Fig. 6C–D). Interestingly, the inhibition of SIRT-2 gene expression rescues cells from αsyn-mediated toxicity in PD (Garske et al., 2007; Outeiro et al., 2007). This result is of particular relevance since several studies based on *in vivo* and *in vitro* experiments have demonstrated that the deletion of SIRT-2 presents a neuroprotective effect. From a mechanistic point of view, SIRT-2 interacts and removes acetyl groups from α-syn, increasing its aggregation and cytotoxicity (de Oliveira et al., 2017; Singh et al., 2021).

Furthermore, HO-1 serves as a defence system against oxidative stress (Yang et al., 2009). Transcription of HO-1 is activated by nuclear factor erythroid 2–related factor 2 (Nrf2) which has a neuroprotective role in Nrf2 signalling in mouse PD models, and an increase in HO-1 protein leads to degradation of heme molecules, producing biliverdin and bilirubin (Motterlini et al., 2002; Jain and Jaiswal, 2006). The accumulation of bilirubin, a potent antioxidant molecule, is responsible, at least partly, for the neuroprotective effects of HO-1. In these regards, DOPAL, MOPET, and MOPAL significantly decrease HO-1 expression (Fig. 6E–F) and therefore, these compounds do not prevent oxidative stress via this gene.

Molecular chaperones are implicated in the refolding of misfolding proteins or their targeting for degradation via the ubiquitin-proteasome system (UPS) or the autophagy-lysosomal pathway (ALP) (Wickner et al., 1999). Under stress conditions, these roles are carried out by Hsps. In fact, Hsp70 may have a role both in refolding and in degrading misfolded αsyn aggregates, by interfering in their oligomerisation, thus providing protection against αsyn toxicity (Klucken et al., 2006; Ebrahimi-Fakhari et al., 2012). Hsp70 possesses an intrinsically higher binding affinity with αsyn which explains its capacity to reduce oligomer formation and to disassemble α-syn fibrils (Aprile et al., 2017; Tao et al., 2021; Schneider et al., 2021). Accordingly, we have demonstrated that DOPAL and MOPET (0.5, 2, 5, 10, and 15 μM) in the absence of αsyn fibrils (Fig. 6G), and DOPAL (0.5, 2, and 5 μM) and MOPET (10 and 15 μM) in their presence (Fig. 6H) significantly increase Hsp70 gene expression (Fig. 6G–H). This fact could be related to the protective effect observed for both compounds. Our data show that DOPAL exerts a protective effect through the vitagene system that has not been previously reported.

In summary, this work revealed that DOPAL is the most potent metabolite, among the studied compounds, for preventing αsyn-fibril formation and destabilising αsyn fibrils. Based on these findings, we can state that the inhibitory and destabilising effect of DOPAL against αsyn fibrils depends not only on DOPAL concentration, but also on the level of protein aggregation.

In addition, our results show that DOPAL, at near physiological concentrations, can protect neurons from αsyn-induced toxicity. Furthermore, the role of DOPAL, MOPET, and MOPAL in the expression of vitagenes has been studied. Thus, the present results show that several mechanisms may be involved in the action of these metabolites against αsyn toxicity. These data contribute to a better understanding of the role of HT and DA metabolites against some of the most important physiopathological processes involved in PD. However, more *in vivo* studies are necessary to sufficiently explore their concentrations in the brain after dietary intervention and their interconversion with DA and HT metabolites.

CRediT authorship contribution statement

Marta Gallardo-Fernández: Investigation, Methodology, Data curation, Formal analysis, Visualization, Writing – original draft, preparation. **Ruth Hornedo-Ortega:** Conceptualization, Investigation, Methodology, Data curation, Formal analysis, Supervision, Visualization, Writing – original draft, preparation and Review, Writing – review & editing. **Ana B. Cerezo:** Conceptualization, Investigation, Data curation, Formal analysis, Supervision, Visualization, Writing – original draft, preparation and Review, Writing – review & editing. **Ana M. Troncoso:** Conceptualization, Investigation, Formal analysis, Project administration, Resources, Supervision, Visualization, Writing – original draft, preparation and Review, Writing – review & editing. **M. Carmen Garcia-Parrilla:** Conceptualization, Investigation, Formal analysis, Project administration, Resources, Supervision, Visualization, Writing – original draft, preparation and Review, Writing – review & editing.

Declaration of competing interest

The authors declare that they have no known competing financial interests or personal relationships that could have appeared to influence the work reported in this paper.

Data availability

Data will be made available on request.

Acknowledgements

The authors are very grateful to the Spanish Government for its financial assistance (Plan Estatal 2017–2020, Ministerio de Ciencia, Innovación y Universidades, Project MICINN PID2019-108722RB-C32), Ministerio de Economía y Competitividad for the predoctoral fellowship (M.G.-F.' FPI contract) and R.H.O′ postdoctoral contract (Ayuda IJC2020-045695-I financed by MCIN/AEI/10.13039/501100011033 and by European Union NextGeneration EU/PRTR).

Appendix A. Supplementary data

Supplementary data to this article can be found online at https://doi.org/10.1016/j.fct.2022.113542.

References

Alcalay, R.N., Gu, Y., Mejia-Santana, H., Cote, L., Marder, K.S., Scarmeas, N., 2012. The association between Mediterranean diet adherence and Parkinson's disease. Mov. Disord. 27, 771–774. https://doi.org/10.1002/mds.24918.

Ambra, R., Natella, F., Bello, C., Lucchetti, S., Forte, V., Pastore, G., 2017. Phenolics fate in table olives (Olea europaea L. cv. Nocellara del Belice) debittered using the Spanish and Castelvetrano methods. Food Res. Int. 100, 369–376. https://doi.org/10.1016/j.foodres.2017.07.027.

Aprile, F.A., Källstig, E., Limorenko, G., Vendruscolo, M., Ron, D., Hansen, C., 2017. The molecular chaperones DNAJB6 and Hsp70 cooperate to suppress α-synuclein aggregation. Sci. Rep. 7, 1–11. https://doi.org/10.1038/s41598-017-08324-z.

Ardah, M.T., Paleologou, K.E., Lv, G., Abul Khair, S.B., Kazim, A.S., Minhas, S.T., Al-Tel, T.H., Al-Hayani, A.A., Haque, M.E., Eliezer, D., El-Agnaf, O., 2014. Structure activity relationship of phenolic acid inhibitors of α-synuclein fibril formation and toxicity. Front. Neurosci. 6, 197. https://doi.org/10.3389/fnagi.2014.00197.

Aaseth, J., Dusek, P., Roos, P.M., 2018. Prevention of progression in Parkinson's disease. Biometals 315, 737–747. https://doi.org/10.1007/s10534-018-0131-5.

Bieschke, J., Russ, J., Friedrich, R.P., Ehrnhoefer, D.E., Wobst, H., Neugebauer, K., Wanker, E.E., 2010. EGCG remodels mature α-synuclein and amyloid-β fibrils and reduces cellular toxicity. Proc. Natl. Acad. Sci. USA 107, 7710–7715. https://doi.org/10.1073/pnas.091072310.

Boselli, E., Minardi, M., Giomo, A., Frega, N.G., 2006. Phenolic composition and quality of white doc wines from Marche (Italy). Anal. Chim. Acta 563, 93–100. https://doi.org/10.1016/j.aca.2005.10.024.

Brunetti, G., Di Rosa, G., Scuto, M., Leri, M., Stefani, M., Schmitz-Linneweber, C., Calabrese, V., Saul, N., 2020. Healthspan maintenance and prevention of

Parkinson's-like phenotypes with hydroxytyrosol and oleuropein aglycone in C. elegans. Int. J. Mol. Sci. 21, 2588. https://doi.org/10.3390/ijms21072588.
Burke, W.J., Chung, H.D., Li, S.W., 1999. Quantitation of 3, 4-dihydroxyphenylacetaldehyde and 3, 4-dihydroxyphenylglycolaldehyde, the monoamine oxidase metabolites of dopamine and noradrenaline, in human tissues by microcolumn high-performance liquid chromatography. Anal. Biochem. 273, 111–116. https://doi.org/10.1006/abio.1999.4196.
Burke, W.J., Kumar, V.B., Pandey, N., Panneton, W.M., Gan, Q., Franko, M.W., O'Dell, M., Li, S.W., Pan, Y., Chung, H.D., Galvin, J.E., 2008. Aggregation of α-synuclein by DOPAL, the monoamine oxidase metabolite of dopamine. Acta Neuropathol. 115, 193–203. https://doi.org/10.1007/s00401-007-0303-9.
Calabrese, V., Stella, A.G., Butterfield, D.A., Scapagnini, G., 2004. Redox regulation in neurodegeneration and longevity: role of the heme oxygenase and HSP70 systems in brain stress tolerance. Antioxidants Redox Signal. 6, 895–913. https://doi.org/10.1089/ars.2004.6.895.
Calabrese, V., Cornelius, C., Dinkova-Kostova, A.T., Calabrese, E.J., 2009. Vitagenes, cellular stress response, and acetylcarnitine: relevance to hormesis. Biofactors 35, 146–160. https://doi.org/10.1002/biof.22.
Calabrese, V., Cornelius, C., Dinkova-Kostova, A.T., Calabrese, E.J., Mattson, M.P., 2010. Cellular stress responses, the hormesis paradigm, and vitagenes: novel targets for therapeutic intervention in neurodegenerative disorders. Antioxidants Redox Signal. 13, 1763–1811. https://doi.org/10.1089/ars.2009.3074.
Carmo-Gonçalves, P., do Nascimento, L.A., Cortines, J.R., Eliezer, D., Romão, L., Follmer, C., 2018. Exploring the role of methionine residues on the oligomerization and neurotoxic properties of DOPAL-modified α-synuclein. Biochem. Biophys. Res. Commun. 505, 295–301. https://doi.org/10.1016/j.bbrc.2018.09.111.
Carmo-Gonçalves, P., Romão, L., Follmer, C., 2020. In vitro protective action of monomeric and fibrillar α-synuclein on neuronal cells exposed to the dopaminergic toxins salsolinol and DOPAL. CS Chem. Neurosci. 11, 3541–3548. https://doi.org/10.1021/acschemneuro.0c00527.
Cioffi, G., Pesca, M.S., De Caprariis, P., Braca, A., Severino, L., De Tommasi, N., 2010. Phenolic compounds in olive oil and olive pomace from Cilento (Campania, Italy) and their antioxidant activity. Food Chem. 121, 105–111. https://doi.org/10.1016/j.foodchem.2009.12.013.
De Oliveira, R.M., Vicente Miranda, H., Francelle, L., Pinho, R., Szegö, É.M., Martinho, R., Munari, F., Lázaro,Sébastien, D.F., Moniot, S., Guerreiro, P., et al., 2017. The mechanism of sirtuin 2–mediated exacerbation of alpha-synuclein toxicity in models of Parkinson disease. PLoS Biol. 15, e2000374 https://doi.org/10.1371/journal.pbio.2000374.
Di Tommaso, D., Calabrese, R., Rotilio, D., 1998. Identification and quantitation of hydroxytyrosol in Italian wines. J. High Resolut. Chromatogr. 21, 549–553. https://doi.org/10.1002/(SICI)1521-4168(19981001)21:10<549::AID-JHRC549>3.0.CO;2-Z.
Dowding, C.H., Shenton, C.L., Salek, S.S., 2006. A review of the health-related quality of life and economic impact of Parkinson's disease. Drugs Aging 23, 693–721. https://doi.org/10.2165/00002512-200623090-00001.
Ebrahimi-Fakhari, D., Wahlster, L., McLean, P.J., 2012. Protein degradation pathways in Parkinson's disease: curse or blessing. Acta Neuropathol. 124, 153–172. https://doi.org/10.1007/s00401-012-1004-6.
Fahn, S., Sulzer, D., 2004. Neurodegeneration and neuroprotection in Parkinson disease. NeuroRx. 1, 139–154. https://doi.org/10.1602/neurorx.1.1.139.
Follmer, C., Coelho-Cerqueira, E., Yatabe-Franco, D.Y., Araujo, G.D., Pinheiro, A.S., Domont, G.B., Eliezer, D., 2015. Oligomerization and membrane-binding properties of covalent adducts formed by the interaction of α-synuclein with the toxic dopamine metabolite 3, 4-dihydroxyphenylacetaldehyde (DOPAL). J. Appl. Biol. Chem. 290, 27660–27679. https://doi.org/10.1074/jbc.M115.686584.
Gallardo-Fernández, M., Hornedo-Ortega, R., Cerezo, A.B., Troncoso, A.M., García-Parrilla, M.C., 2019. Melatonin, protocatechuic acid and hydroxytyrosol effects on vitagenes system against alpha-synuclein toxicity. Food Chem. Toxicol. 134, 110817 https://doi.org/10.3390/antiox9010036.
Gao, B., Kong, Q., Kemp, K., Zhao, Y.S., Fang, D., 2012. Analysis of sirtuin 1 expression reveals a molecular explanation of IL-2–mediated reversal of T-cell tolerance. Proc. Natl. Acad. Sci. USA 109, 899–904. https://doi.org/10.1073/pnas.1118462109.
Garske, A.L., Smith, B.C., Denu, J.M., 2007. Linking SIRT2 to Parkinson's disease. ACS Chem. Biol. 2, 529–532. https://doi.org/10.1021/cb700160d.
Giovanni, G.D., Esposito, E., Matteo, V.D., 2009. In vivo microdialysis in Parkinson's research. Birth, life and death of dopaminergic neurons in the substantia nigra. J. Neural. Transm. Suppl. 223–243. https://doi.org/10.1007/978-3-211-92660-4.
Goedert, M., 2001. Parkinsons Disease and other α-Synucleinopathies. Clin. Chem. Lab. Med. 39, 308–312. https://doi.org/10.1515/CCLM.2001.047.
Goldstein, D.S., 2020. The catecholaldehyde hypothesis: where MAO fits in. J. Neural. Transm. 127, 169–177. https://doi.org/10.1007/s00702-019-02106-9.
Hornedo-Ortega, R., Alvarez-Fernandez, M.A., Cerezo, A.B., Richard, T., Troncoso, A.M., Garcia-Parrilla, M.C., 2016. Protocatechuic acid: inhibition of fibril formation, destabilization of preformed fibrils of amyloid-β and α-synuclein, and neuroprotection. J. Agric. Food Chem. 64, 7722–7732. https://doi.org/10.1021/acs.jafc.6b03217.
Hornedo-Ortega, R., Cerezo, A.B., Troncoso, A.M., Garcia-Parrilla, M.C., 2018a. Protective effects of hydroxytyrosol against α-synuclein toxicity on PC12 cells and fibril formation. Food Chem. Toxicol. 120, 41–49. https://doi.org/10.1016/j.fct.2018.06.059.
Hornedo-Ortega, R., Da Costa, G., Cerezo, A.B., Troncoso, A.M., Richard, T., Garcia-Parrilla, M.C., 2018b. In vitro effects of serotonin, melatonin, and other related indole compounds on amyloid-β kinetics and neuroprotection. Mol. Nutr. Food Res. 62, 1700383 https://doi.org/10.1002/mnfr.201700383.
Hornedo-Ortega, R., Jourdes, M., Da Costa, G., Courtois, A., Gabaston, J., Teissedre, P.L., Richard, T., Krisa, S., 2022. Oxyresveratrol and gnetol glucuronide metabolites: chemical production, structural identification, metabolism by human and rat liver fractions, and in vitro anti-inflammatory properties. J. Agric. Food Chem. 70 (41), 13082–13092. https://doi.org/10.1021/acs.jafc.1c07831.
Jain, A.K., Jaiswal, A.K., 2006. Phosphorylation of tyrosine 568 controls nuclear export of Nrf2. J. Appl. Biol. Chem. 281, 12132–12142. https://doi.org/10.1074/jbc.M511198200.
Jones, D.R., Moussaud, S., McLean, P., 2014. Targeting heat shock proteins to modulate α-synuclein toxicity. Ther. Adv. Chronic Dis. 7, 33–51. https://doi.org/10.1177/1756285613493469.
Johnson, R., Melliou, E., Zweigenbaum, J., Mitchell, A.E., 2018. Quantitation of oleuropein and related phenolics in cured Spanish-style green, California-style black ripe, and Greek-style natural fermentation olives. J. Agric. Food Chem. 66, 2121–2128. https://doi.org/10.1021/acs.jafc.7b06025.
Kesen, S., Kelebek, H., Selli, S., 2013. Characterization of the volatile, phenolic and antioxidant properties of monovarietal olive oil obtained from cv. Halhali. J. Am. Oil Chem. 90, 1685–1696. https://doi.org/10.1007/s11746-013-2327-8.
Kim, D., Nguyen, M.D., Dobbin, M.M., Fischer, A., Sananbenesi, F., Rodgers, J.T., Delalle, I., Baur, J.A., Sui, G., Armour, S.M., Puigserver, P., Sinclair, D.A., Tsai, L.H., 2007. SIRT1 deacetylase protects against neurodegeneration in models for Alzheimer's disease and amyotrophic lateral sclerosis. EMBO J. 26, 3169–3179. https://doi.org/10.1038/sj.emboj.7601758.
Klucken, J., Ingelsson, M., Shin, Y., Irizarry, M.C., Hedley-Whyte, E.T., Frosch, M., Growdon, J., Mclean, P., Hyman, B.T., 2006. Clinical and biochemical correlates of insoluble α-synuclein in dementia with Lewy bodies. Acta Neuropathol. 111, 101–108. https://doi.org/10.1007/s00401-005-0027-7.
Kristal, B.S., Conway, A.D., Brown, A.M., Jain, J.C., Ulluci, P.A., Li, S.W., Burke, W.J., 2001. Selective dopaminergic vulnerability: 3, 4-dihydroxyphenylacetaldehyde targets mitochondria. Free Radic. Biol. Med. 30, 924–931. https://doi.org/10.1016/S0891-5849(01)00484-1.
Lambert, J.D., Sang, S., Yang, C.S., 2007. Biotransformation of green tea polyphenols and the biological activities of those metabolites. Mol. Pharm. 4, 819–825. https://doi.org/10.1021/mp700075m.
Larrosa, M., Luceri, C., Vivoli, E., Pagliuca, C., Lodovici, M., Moneti, G., Dolara, P., 2009. Polyphenol metabolites from colonic microbiota exert anti-inflammatory activity on different inflammation models. Mol. Nutr. Food Res. 53, 1044–1054. https://doi.org/10.1002/mnfr.200800446.
Lima, V.D.A., do Nascimento, L.A., Eliezer, D., Follmer, C., 2018. Role of Parkinson's disease-linked mutations and N-terminal acetylation on the oligomerization of α-synuclein induced by 3, 4-dihydroxyphenylacetaldehyde. ACS Chem. Neurosci. 10, 690–703. https://doi.org/10.1021/acschemneuro.8b00498.
López de las Hazas, M.C.L., Piñol, C., Macià, A., Romero, M.P., Pedret, A., Solà, R., Rubió, L., Motilva, M.J., 2016. Differential absorption and metabolism of hydroxytyrosol and its precursors oleuropein and secoiridoids. J. Funct.Foods 22, 52–63. https://doi.org/10.1016/j.jff.2016.01.030.
López de las Hazas, M.C.L., Godinho-Pereira, J., Macià, A., Almeida, A.F., Ventura, M.R., Motilva, M.J., Santos, C.N., 2018. Brain uptake of hydroxytyrosol and its main circulating metabolites: protective potential in neuronal cells. J. Funct.Foods 46, 110–117. https://doi.org/10.1016/j.jff.2018.04.028.
Macario, A.J., De Macario, E.C., 2007. Chaperonopathies by defect, excess, or mistake. Ann. N. Y. Acad. Sci. 1113, 178–191. https://doi.org/10.1196/annals.1391.009.
Mancuso, C., 2004. Heme oxygenase and its products in the nervous system. Redox Signal 6, 878–887. https://doi.org/10.1089/ars.2004.6.878.
Meiser, J., Weindl, D., Hiller, K., 2013. Complexity of dopamine metabolism. J. Cell Commun. Signal. 11, 1–18. https://doi.org/10.1186/1478-811X-11-34.
Mencacci, N.E., Isaias, I.U., Reich, M.M., Ganos, C., Plagnol, V., Polke, J.M., Bras, J., Herheson, J., Stamelou, M., Pittman, A.M., Noyce, A.J., Mok, K.Y., Opladen, T., et al., 2014. Parkinson's disease in GTP cyclohydrolase 1 mutation carriers. Brain 137, 2480–2492. https://doi.org/10.1093/brain/awu179.
Monzani, E., Nicolis, S., Dell'Acqua, S., Capucciati, A., Bacchella, C., Zucca, F.A., Mosharov, E.V., Sulzer, D., Zecca, L., Casella, L., 2019. Dopamine, oxidative stress and protein–quinone modifications in Parkinson's and other neurodegenerative diseases. Angew. Chem. Int. Ed. 58, 6512–6527. https://doi.org/10.1002/anie.201811122.
Morimoto, R., 2014. Creating a path from the heat shock response to therapeutics of protein-folding diseases: an interview with Rick Morimoto. Dis. Model. Mech. 7, 5–8. https://doi.org/10.1242/dmm.014753.
Motterlini, R., Green, C.J., Foresti, R., 2002. Regulation of heme oxygenase-1 by redox signals involving nitric oxide. Antioxidants Redox Signal. 4, 615–624. https://doi.org/10.1089/15230860260220111.
Muñoz, P., Huenchuguala, S., Paris, I., Segura-Aguilar, J., 2012. Dopamine oxidation and autophagy. Parkinsons Dis. https://doi.org/10.1155/2012/920953, 2012.
Ng, F., Wijaya, L., Tang, B.L., 2015. SIRT1 in the brain—connections with aging-associated disorders and lifespan. Front. Cell. Neurosci. 9, 64. https://doi.org/10.3389/fncel.2015.00064.
Ono, K., Mochizuki, H., Ikeda, T., Nihira, T., Takasaki, J.I., Teplow, D.B., Yamada, M., 2012. Effect of melatonin on α-synuclein self-assembly and cytotoxicity. Neurobiol. Aging 33, 2172–2185. https://doi.org/10.1016/j.neurobiolaging.2011.10.015.
Othman, N.B., Roblain, D., Chammen, N., Thonart, P., Hamdi, M., 2009. Antioxidant phenolic compounds loss during the fermentation of Chétoui olives. Food Chem. 116, 662–669. https://doi.org/10.1016/j.foodchem.2009.02.084.
Outeiro, T.F., Kontopoulos, E., Altmann, S.M., Kufareva, I., Strathearn, K.E., Amore, A.M., Volk, C.B., Maxwell, M.M., Rochet, J.C., McLean, P.J., et al., 2007. Sirtuin 2 inhibitors rescue α-synuclein-mediated toxicity in models of Parkinson's disease. Science 317, 516–519. https://doi.org/10.1126/science.1143780.

Palazzi, L., Bruzzone, E., Bisello, G., Leri, M., Stefani, M., Bucciantini, M., Polverino de Laureto, P., 2018. Oleuropein aglycone stabilizes the monomeric α-synuclein and favours the growth of non-toxic aggregates. Sci. Rep. 8, 1–17. https://doi.org/10.1038/s41598-018-26645-5.

Palazzi, L., Leri, M., Cesaro, S., Stefani, M., Bucciantini, M., de Laureto, P.P., 2020. Insight into the molecular mechanism underlying the inhibition of α-synuclein aggregation by hydroxytyrosol. Biochem. Pharmacol. 173, 113722 https://doi.org/10.1016/j.bcp.2019.113722.

Pereira, J.A., Pereira, A.P., Ferreira, I.C., Valentão, P., Andrade, P.B., Seabra, R., Estevinho, L., Bento, A., 2006. Table olives from Portugal: phenolic compounds, antioxidant potential, and antimicrobial activity. J. Agric. Food Chem. 54, 8425–8431. https://doi.org/10.1021/jf061769j.

Pérez-Barrón, G., Montes, S., Aguirre-Vidal, Y., Santiago, M., Gallardo, E., Espartero, J.L., Ríos, C., Monroy-Noyola, A., 2021. Antioxidant effect of hydroxytyrosol, hydroxytyrosol acetate and nitrohydroxytyrosol in a rat MPP+ model of Parkinson's disease. Neurochem. Res. 46, 2923–2935. https://doi.org/10.1007/s11064-021-03379-x.

Piñeiro, Z., Cantos-Villar, E., Palma, M., Puertas, B., 2011. Direct liquid chromatography method for the simultaneous quantification of hydroxytyrosol and tyrosol in red wines. J. Agric. Food Chem. 59, 11683–11689. https://doi.org/10.1021/jf202254t.

Plotegher, N., Berti, G., Ferrari, E., Tessari, I., Zanetti, M., Lunelli, L., Greggio, E., Bisaglia, M., Veronesi, M., Girotto, S., et al., 2017. DOPAL derived alpha-synuclein oligomers impair synaptic vesicles physiological function. Sci. Rep. 7, 1–16. https://doi.org/10.1038/srep40699.

Proestos, C., Bakogiannis, A., Psarianos, C., Koutinas, A.A., Kanellaki, M., Komaitis, M., 2005. High performance liquid chromatography analysis of phenolic substances in Greek wines. Food Control 16, 319–323. https://doi.org/10.1016/j.foodchem.2004.12.016.

Rodríguez-Morató, J., Boronat, A., Kotronoulas, A., Pujadas, M., Pastor, A., Olesti, E., Pérez-Mañá, C., Khymenets, O., Fitó, M., Farré, M., De la Torre, R., 2016. Metabolic disposition and biological significance of simple phenols of dietary origin: hydroxytyrosol and tyrosol. Drug Metab. Rev. 48, 218–236. https://doi.org/10.1080/03602532.2016.1179754.

Scarmeas, N., Stern, Y., Mayeux, R., Manly, J.J., Schupf, N., Luchsinger, J.A., 2009. Mediterranean diet and mild cognitive impairment. Arch. Neurol. 66, 216–225. https://doi.org/10.1001/archneurol.2008.536.

Schneider, M.M., Gautam, S., Herling, T.W., Andrzejewska, E., Krainer, G., Miller, A.M., Trinkaus, V.A., Peter, A.E., Simone Ruggeri, F., Vendruscolo, M., et al., 2021. The Hsc70 disaggregation machinery removes monomer units directly from α-synuclein fibril ends. Nat. Commun. 12, 1–11. https://doi.org/10.1038/s41467-021-25966-w.

Singh, P., Hanson, P.S., Morris, C.M., 2017. SIRT1 ameliorates oxidative stress induced neural cell death and is down-regulated in Parkinson's disease. BMC Neurosci. 18, 1–13. https://doi.org/10.1186/s12868-017-0364-1.

Singh, A.P., Nigam, L., Yadav, Y., Shekhar, S., Subbarao, N., Dey, S., 2021. Design and in vitro analysis of SIRT2 inhibitor targeting Parkinson's disease. Mol. Divers. 25, 2261–2270. https://doi.org/10.1007/s11030-020-10116-z.

Srivastava, S., Haigis, M.C., 2011. Role of sirtuins and calorie restriction in neuroprotection: implications in Alzheimer's and Parkinson's diseases. Curr. Pharmaceut. Des. 17, 3418–3433. https://doi.org/10.2174/138161211798072526.

Steiner, J.A., Angot, E., Brundin, P., 2011. A deadly spread: cellular mechanisms of α-synuclein transfer. Cell Death Dis. 18, 1425–1433. https://doi.org/10.1038/cdd.2011.53.

Tao, J., Berthet, A., Citron, Y.R., Tsiolaki, P.L., Stanley, R., Gestwicki, J.E., Agard, D.A., McConlogue, L., 2021. Hsp70 chaperone blocks α-synuclein oligomer formation via a novel engagement mechanism. J. Biol. Chem. 296 https://doi.org/10.1016/j.jbc.2021.100613.

Trovato Salinaro, A., Cornelius, C., Koverech, G., Koverech, A., Scuto, M., Lodato, F., Fronte, V., Muccilli, V., Reibaldi, M., Longo, A., et al., 2014. Cellular stress response, redox status, and vitagenes in glaucoma: a systemic oxidant disorder linked to Alzheimer's disease. Front. Med. 5, 129. https://doi.org/10.3389/fphar.2014.00129.

Twelves, D., Perkins, K.S., Counsell, C., 2003. Systematic review of incidence studies of Parkinson's disease. Mov. Disord. 18, 19–31. https://doi.org/10.1002/mds.10305.

Vissers, M.N., Zock, P.L., Roodenburg, A.J., Leenen, R., Katan, M.B., 2002. Olive oil phenols are absorbed in humans. Nutr. J. 132, 409–417. https://doi.org/10.1093/jn/132.3.409.

Werner-Allen, J.W., DuMond, J.F., Levine, R.L., Bax, A., 2016. Toxic dopamine metabolite DOPAL forms an unexpected dicatechol pyrrole adduct with lysines of α synuclein. Angew. Chem. Int. Ed. 55, 7374–7378. https://doi.org/10.1002/anie.201600277.

Wickner, S., Maurizi, M.R., Gottesman, S., 1999. Posttranslational quality control: folding, refolding, and degrading proteins. Science 286, 1888–1893. https://doi.org/10.1126/science.286.5446.1888.

Winner, B., Jappelli, R., Maji, S.K., Desplats, P.A., Boyer, L., Aigner, S., Hetzer, C., Loher, T., Vilar, M., Campioni, S., et al., 2011. In vivo demonstration that α-synuclein oligomers are toxic. Proc. Natl. Acad. Sci. USA 108, 4194–4199. https://doi.org/10.1073/pnas.1100976108.

Wu, Y.T., Lin, L.C., Tsai, T.H., 2009. Measurement of free hydroxytyrosol in microdialysates from blood and brain of anesthetized rats by liquid chromatography with fluorescence detection. J. Chromatogr. A 1216, 3501–3507. https://doi.org/10.1016/j.chroma.2008.10.116.

Xu, J., Kao, S.Y., Lee, F.J., Song, W., Jin, L.W., Yankner, B.A., 2002. Dopamine-dependent neurotoxicity of α-synuclein: a mechanism for selective neurodegeneration in Parkinson disease. Nat. Med. 8, 600–606. https://doi.org/10.1038/nm0602-600.

Yang, S., Hu, S., Chen, J., Choudhry, M.A., Rue III, L.W., Bland, K.I., Chaudry, I.H., 2009. Mechanism of hepatoprotection in proestrus female rats following trauma-hemorrhage: heme oxygenase-1-derived normalization of hepatic inflammatory responses. J. Leukoc. Biol. 85, 1015–1026. https://doi.org/10.1189/jlb.0508288.

Further reading

Gallardo-Fernández, M., Cerezo, A.B., Hornedo-Ortega, R., Troncoso, A.M., Garcia-Parrilla, M.C., 2022. Anti-VEGF effect of bioactive indolic compounds and hydroxytyrosol metabolites. Foods 11, 526. https://doi.org/10.3390/foods11040526.